Toxicology 339 (2016) 73–86

Contents lists available at ScienceDirect

Toxicology

journal homepage: www.elsevier.com/locate/toxicol

Systems toxicology-based assessment of the candidate modified risk tobacco product THS2.2 for the adhesion of monocytic cells to human coronary arterial endothelial cells

Carine Poussin*, Alexandra Laurent, Manuel C. Peitsch, Julia Hoeng, Hector De Leon

Philip Morris International R&D, Philip Morris Products S.A., Quai Jeanrenaud 5, 2000 Neuchâtel, Switzerland

ARTICLE INFO

Article history:
Received 20 October 2015
Received in revised form 26 November 2015
Accepted 30 November 2015
Available online 2 December 2015

Keywords:
Modified risk tobacco product
Cigarette
Monocyte
Endothelial cell
Adhesion
Atherosclerosis

ABSTRACT

Alterations of endothelial adhesive properties by cigarette smoke (CS) can progressively favor the development of atherosclerosis which may cause cardiovascular disorders. Modified risk tobacco products (MRTPs) are tobacco products developed to reduce smoking-related risks. A systems biology/toxicology approach combined with a functional in vitro adhesion assay was used to assess the impact of a candidate heat-not-burn technology-based MRTP, Tobacco Heating System (THS) 2.2, on the adhesion of monocytic cells to human coronary arterial endothelial cells (HCAECs) compared with a reference cigarette (3R4F). HCAECs were treated for 4 h with conditioned media of human monocytic Mono Mac 6 (MM6) cells preincubated with low or high concentrations of aqueous extracts from THS2.2 aerosol or 3R4F smoke for 2 h (indirect treatment), unconditioned media (direct treatment), or fresh aqueous aerosol/smoke extracts (fresh direct treatment). Functional and molecular investigations revealed that aqueous 3R4F smoke extract promoted the adhesion of MM6 cells to HCAECs via distinct direct and indirect concentration-dependent mechanisms. Using the same approach, we identified significantly reduced effects of aqueous THS2.2 aerosol extract on MM6 cell-HCAEC adhesion, and reduced molecular changes in endothelial and monocytic cells. Ten- and 20-fold increased concentrations of aqueous THS2.2 aerosol extract were necessary to elicit similar effects to those measured with 3R4F in both fresh direct and indirect exposure modalities, respectively. Our systems toxicology study demonstrated reduced effects of an aqueous aerosol extract from the candidate MRTP, THS2.2, using the adhesion of monocytic cells to human coronary endothelial cells as a surrogate pathophysiologically relevant event in atherogenesis.

© 2015 Z. Published by Elsevier Ireland Ltd. This is an open access article under the CC BY-NC-ND license (http://creativecommons.org/licenses/by-nc-nd/4.0/).

1. Introduction

Smoking is a major risk factor for the development of cardiovascular diseases (Messner and Bernhard 2014). Cigarette smoke (CS) contains constituents that cross the alveolar barrier into the blood stream, elicit systemic effects, and affect peripheral organs and tissues such as blood vessels and the heart distal from the lungs. Over time, smokers develop low grade inflammatory, (e.g., release of cytokines and eicosanoids) and pro-oxidative (e.g., oxidized low-density lipoprotein) features in the blood that can affect normal vascular regulatory functions including vasotone regulation, endothelial permeability, and coagulation. These changes favor and accelerate the appearance of atherosclerotic plaques (Favero et al., 2014; Messner and Bernhard 2014; Yanbaeva et al., 2007).

The development of innovative modified risk tobacco products (MRTPs) that reduce the incidence of cardiovascular and other smoking-related diseases (e.g., lung diseases), and subsequently decrease the morbidity and mortality of smoking is necessary for public health concerns (Administration, 2012b). CS contains thousands of toxic chemicals, including acrolein, benzene, and cadmium (Haussmann, 2012; Perfetti and Rodgman, 2011; Rodgman and Perfetti, 2013). However, by heating rather than burning tobacco it is possible to markedly decrease the amount of harmful constituents in the aerosol (e.g., including, but not limited to,

Abbreviations: CS, cigarette smoke; FDR, false discovery rate; HCAECs, human coronary artery endothelial cells; I, D, and FD, indirect, direct and fresh direct, respectively; ICAM-1, intercellular adhesion molecule 1; MM6, Mono Mac 6; MRTP, modified risk tobacco product; NPA, network perturbation amplitude; (R)BIF, (Relative) biological impact factor; SELE, E-selectin; SM, starvation medium; TACE, tumor necrosis factor-α-converting enzyme; THS2.2, Tobacco Heating System 2.2; TNFα, tumor necrosis factor-alpha; TRAG, tissue repair and angiogenesis network; VCAM-1, vascular cell adhesion molecule 1; V-IPN, vascular-inflammatory processes network; IPN, inflammatory processes.

* Corresponding author. Fax: +41 58 242 2811.
E-mail address: Carine.Poussin@pmi.com (C. Poussin).

http://dx.doi.org/10.1016/j.tox.2015.11.007
0300-483X/© 2015 Z. Published by Elsevier Ireland Ltd. This is an open access article under the CC BY-NC-ND license (http://creativecommons.org/licenses/by-nc-nd/4.0/).

aldehydes and polycyclic aromatic hydrocarbons) (Schorp et al., 2012; Werley et al., 2008). Recent investigations into the biological impact of a heat-not-burn technology-based prototypic (p) MRTP have shown reduced exposure effects compared with those observed with a reference cigarette. For instance, a 7-month smoke inhalation study reported significant reductions of inflammation and emphysema in the lungs of mice exposed to pMRTP (carbon-heated tobacco technology) compared with a 3R4F reference cigarette at matching nicotine concentrations (Phillips et al., 2015). Diminished inflammatory and oxidative stress responses were also measured in nasal and bronchial epithelia, and lung parenchyma of rats exposed to pMRTP aerosol for 28 days (Kogel et al., 2014). Regarding the cardiovascular system, a recent in vitro study showed that the aqueous extract of a pMRTP (smoke-bubbled media) exhibited reduced effects on chemotaxis and the transendothelial migration of monocytes compared with the 3R4F reference cigarette (van der Toorn et al., 2015b).

CS has been shown to modify the adhesive properties of the endothelium, leading to higher rates of leukocyte–endothelial cell adhesion (Winkelmann et al., 2009). Mechanistic studies from our group and others have reported direct and indirect effects of CS on monocyte–endothelial cell adhesion promoted by the increased expression of adhesion proteins at the surface of endothelial cells (Kalra et al., 1994; Lehr 1993; Poussin et al., 2014; Wang et al., 2004; Zhang et al., 2002). The direct effect of CS was reported to be mediated by the direct influence of CS constituents on endothelial cells, while the indirect effect was described to be driven via the paracrine inflammatory effect of soluble mediators secreted by CS-treated monocytic cells (Poussin et al., 2014; Zhang et al., 2002).

Current literature findings diverge with regards to direct and indirect effects of CS on monocyte-endothelium adhesion, which may reflect the heterogeneity of experimental set ups (e.g., exposure time, types of CS fractions and cellular systems) and may capture the aspects of different mechanisms. To mechanistically investigate the direct and indirect effects of aqueous 3R4F smoke extracts on the adhesion of monocytes to endothelial cells, we previously established an in vitro adhesion assay combined with a comprehensive computational transcriptomics data analysis approach (Poussin et al., 2015). We identified that, at low 3R4F smoke extract concentrations, monocyte–endothelial cell adhesion was promoted indirectly by an inflammatory response in human coronary arterial endothelial cells (HCAECs) induced by soluble mediators secreted by Mono Mac 6 (MM6) cells preexposed to aqueous 3R4F smoke extract (indirect treatment, I). We discovered that tumor necrosis factor (TNF)α, one of the main drivers of the MM6 cell-HCAEC adhesion was enzymatically shed from the MM6 cell surface by TNFα-converting enzyme (TACE) activated by a subset of unstable CS constituents (possibly reactive oxygen species, ROS) present in the medium. When HCAECs were exposed to a high concentration of fresh aqueous 3R4F smoke fraction (fresh direct treatment, FD), MM6 cell-HCAEC adhesion occurred directly via a different mechanism associated with cytotoxic effects induced by another subset of CS constituents that were unstable upon aging and freeze/thaw cycle (Poussin et al., 2015). Although the FD condition may be less physiologically relevant than the I one, it remains important to expose the system to conditions that induce toxicological effects and gain mechanistic insights in vitro. Unstable CS constituents, present in whole smoke, may interact and be metabolized in lung cells such as bronchial epithelial cells and alveolar macrophages before entering the circulation with modified functional properties. Despite some limitations, the indirect condition mimics exposure of the endothelial cell monolayer to inflammatory mediators released by other cells exposed to CS as well as low concentrations of stable CS-derived constituents or metabolites. In vivo, chronic exposure to low concentrations of inflammatory molecules concomitant with oxidants present in circulating blood plasma modifies endothelial functions, and favors the formation of atherosclerosis (Favero et al., 2014; Messner and Bernhard, 2014; Yanbaeva et al., 2007). Leveraging a previously established experimental and computational framework (Poussin et al., 2015), the present study aimed to compare the biological impact of aqueous extracts from a candidate MRTP, Tobacco Heating System (THS) 2.2 (electrically-heated tobacco technology), and the 3R4F reference cigarette on monocytic cell-HCAEC adhesion combining functional measurements from an in vitro adhesion assay with transcriptomics and inflammatory protein marker data to investigate changes at the molecular level.

2. Material and methods

2.1. Cell culture

HCAECs (Vitaris, Baar, Switzerland) were cultured in collagen A-coated flasks with endothelial cell growth medium MV2 containing 5% fetal calf serum (FCS). MM6 cells (DSMZ, Braunschweig, Germany) were maintained in RPMI 1640 medium (PAA, #E15-0.39, Pashing, Austria) containing 10% FCS, L-glutamine (0.86%), non-essential amino acids (0.86%), oxaloacetate pyruvate insulin media supplement (0.86%, Sigma, #O5003, Buchs, Switzerland) and penicillin/streptomycin (1.7%; Ruwag, # P11-010, Bettlach, Switzerland).

2.2. Preparation of aqueous extracts from THS2.2 aerosol or 3R4F smoke

Mainstream smoke from reference cigarette 3R4F (University of Kentucky) was generated on a 20-port rotary Borgwaldt smoking machine according to the Health Canada standard protocol and bubbled through ice cold phosphate buffered saline (PBS) (6 cigarettes/36 ml PBS, stock solution concentration: ~1.8 puffs/ml; ~10.7 puffs per cigarette in average) at room temperature as described previously (Poussin et al., 2015). The aqueous extract from 3R4F smoke is also often termed as 3R4F smoke-bubbled PBS (sbPBS) (Poussin et al., 2014, 2015).

Mainstream aerosol from the candidate MRTP, THS2.2 developed by Philip Morris international R&D was produced using a predefined puff count of 12 puffs per stick on a 30-port rotary aerosol generator (type SM 2000 P1) according to the Health Canada protocol. The aerosol was bubbled into ice cold PBS to trap the water soluble fraction (10 heatsticks/40 ml, stock solution concentration: 3 puffs/ml).

Final concentrations of 3R4F aqueous extract ranged from 0.06 to 0.225 puffs/ml. Previously, Su et al. (1998) calculated that 2.5% (2.5 cigarettes/l) to 10% (10 cigarettes/l) final concentrations of a 100% cigarette smoke extract PBS stock solution of 100 cigarettes/L (3 cigarettes smoked in 30 ml) corresponded approximately to exposures associated with smoking less than ~0.5–2 packs per day. Therefore, our range of concentrations would correspond to less than 1–4 packs of cigarettes smoked per day. For each experiment, freshly prepared THS2.2 and 3R4F aqueous extract stock solutions were diluted in RPMI 1640 containing 0.5% FCS (starvation medium (SM)), to obtain final aqueous extract concentrations. Vehicle controls corresponded to 15% or 75% (v/v) PBS diluted in starvation medium (Table 1).

2.3. Chemical analysis of aqueous 3R4F smoke and THS2.2 aerosol extracts

2.3.1. Carbonyl concentration determination.

The concentration of eight carbonyls was determined in aqueous extracts by liquid chromatography–electrospray

Table 1
Summary of experimental conditions including cell type, treatment type, items, final selected concentrations, positive and negative controls as well as terminology/abbreviations used in figures.

Cell type	Treatment type	Item	Concentration (puffs/ml)	Terminology/ abbreviations
Mono Mac 6 cells (MM6)	Freshly generated aqueous extract	- 3R4F - THS2.2*	0.045/0.06 0.225 1.125*	3R4F 0.06 3R4F 0.225 THS2.2 0.06 THS2.2 0.225 THS2.2 1.125
	Negative control	PBS (15 or 75% v/v) in SM** (see below)	0	PBS 0
	Positive control	Lipopolysaccharide	1 ug/ml	LPS
Human coronary endothelial cells (HCAECs)	- Indirect (I): conditioned medium# - Direct (D): unconditioned medium# - Fresh direct (FD): freshly generated aqueous extract§	- 3R4F - THS2.2*	0.045/0.06 0.225 1.125#* or 2.25§*	I 3R4F 0.06 I 3R4F 0.225 I THS2.2 0.06 I THS2.2 0.225 I THS2.2 1.125 D 3R4F 0.06 D 3R4F 0.225 D THS2.2 0.06 D THS2.2 0.225 D THS2.2 1.125 FD 3R4F 0.06 FD 3R4F 0.225 FD THS2.2 0.06 FD THS2.2 0.225 FD THS2.2 2.25
	Negative control 1	Starvation medium: RPMI 1640 + 0.5% fetal calf serum (FCS)		SM**
	Negative control 2	- Conditioned medium - Unconditioned medium - PBS (15 or 75% v/v) in SM**	0	I PBS 0 D PBS 0 FD PBS 0
	Positive control	Tumor necrosis factor-alpha	10 ng/ml	TNFA

PBS, phosphate buffered saline.

ionization tandem mass spectrometry (LC–MS) to monitor for batch consistency as previously described (van der Toorn et al., 2015b). Briefly, carbonyl compounds were trapped during the bubbling of 3R4F smoke/THS2.2 aerosol in PBS as described above. Chemical derivatization and quenching were performed to stabilize the carbonyl compounds in the extracts prior to LC–MS analysis. The carbonyl compound concentration expressed as μg/item was calculated using an external calibration curve.

2.3.2. Nicotine concentration determination

Hundred microliter of aqueous extract (100 μl) were added to 400 μl of PBS and 500 μl of ethanol containing the internal standard DL-nicotine-(methyl-d3) in a 2 ml HPLC vial. This sample preparation (5 μl) was injected into a high performance liquid chromatograph coupled to tandem mass spectrometer (HPLC–MS/MS) in multiple reaction monitoring mode using isotope dilution technique. The quantification of nicotine was determined using a 10-point internal standard calibration linear curve.

2.4. Treatment of HCAECs prior to functional and molecular analyses

HCAECs were grown in endothelial cell growth medium MV2 for 24 h in collagen A-coated 96-well plates (Milian, #356649, Niederwil, Switzerland) until 80% confluent. Cells were starved for 24 h in endothelial cell starvation medium containing 0.25% FCS and then treated for 4 h with (Supplementary Fig. 1): (1) conditioned media from MM6 cells preincubated with low or high concentrations of THS2.2 or 3R4F aqueous extracts for 2 h (indirect treatment, I); (2) unconditioned media similarly prepared without MM6 cells (direct treatment, D); or (3) freshly generated THS2.2 or 3R4F aqueous extracts (fresh direct treatment, FD). The preparation of media for I, D, and FD treatments and respective vehicle controls are described in detail (Poussin et al., 2015) and the final concentrations used for 3R4F and THS2.2 are indicated in Table 1. After 4 h treatment, HCAECs in the first plate were used to perform an adhesion assay in vitro, and cells in the second plate were collected, lysed, and frozen for further transcriptomics analysis.

2.5. In vitro adhesion assay

Briefly, HCAECs were stained, at the end of the 4 h treatments, with 1 μg/ml Hoechst 33342 (Sigma, Buchs, Switzerland) for 15 min at 37 °C. Then, 2.5×10^5 freshly Draq5-stained MM6 cells (5 μM Draq5; Brunschwig, Basel, Switzerland) per well were added on top of the stained HCAECs. After 45 min of incubation at 37 °C, the cells were washed three times with PBS and fixed for 15 min with 4% formaldehyde (Sigma, Buchs, Switzerland). Adherent MM6 cells and HCAECs were counted using an ArrayScan (Cellomics, Langenselbold, Germany) as described in Poussin et al. (2015).

2.6. Measurement of inflammatory markers in MM6 cell conditioned media

TNFα levels in MM6 cell conditioned media were measured using an enzyme linked immunosorbent assay (ELISA) kit (R&D Systems, Abingdon, UK). Additionally, a panel of 45 inflammatory markers (Human InflammationMAP® v1.0) was quantified by Myriad–Rules Based Medicine (Austin, TX, USA) using multiplexed immunoassays (multi-analyte profiling).

2.7. RNA preparation and transcriptome analysis

RNA from MM6 and HCAECs (triplicate samples) was extracted and then used for transcritpomics data generation. Further details are available in Poussin et al.'s paper.

2.8. Computational analysis of transcriptomics data

2.8.1. Data processing and pairwise comparisons

Raw data (CEL files with access ID E-MTAB-3923 are available in the ArrayExpress repository database) was processed using GC-Robust Multiarray Average for background correction, probe intensity normalization, and probe-to-probe set intensity summarization (Wu et al., 2004). Quality control analysis of data (e.g., NUSE and RLE plots, pseudo-images, and probe intensity distribution) indicated that all arrays were of good quality. Differential gene expression analysis was performed using the Bioconductor Limma R package (Smyth 2004). Pairwise comparisons, called systems response profiles (SRPs), were computed by comparing each concentration-treatment with its respective vehicle control. For example, the pairwise comparison of HCAECs treated with the conditioned media of MM6 cells pre-exposed to 3R4F aqueous extract (0.06 puffs/ml) versus PBS15% was annotated I 3R4F 0.06. Genes with a false discovery rate (FDR) (*p-value* adjustment using the Benjamini and Hochberg method) below 0.05 were considered differentially expressed genes (DEGs) (Benjamini and Hochberg 1995). SRPs were further leveraged in downstream computational analyses. Data were mapped and collapsed to avoid multiple probe set-to-gene values (Hermida et al., 2013). All R packages (affy, simpleaffy, gcrma, affyPLM, and limma) used to conduct the data analysis were included in Bioconductor 2.13 version. The R version used was 3.1.2.

2.8.2. Network perturbation amplitude (NPA) and biological impact factor (BIF) analysis

Leveraging transcriptomics data and biological cause-and-effect network models, a newly developed computational approach that quantifies a response to any stimulus type while providing mechanistic insights, was applied to analyze network perturbation (Martin et al., 2014) in HCAECs and MM6 cells. Briefly, a network is an assembly of directed and signed causal relationships between molecular biological entities (e.g., protein abundance and activities, chemical compounds, biological activity, and gene expression), which collectively models a specific biological process, such as cell proliferation, inflammation and apoptosis, in a defined context (e.g., lung or vascular). The causal relationships have been manually curated from the scientific literature and encoded in Biological Expression Language syntax. The network is composed of functional (backbone) and transcript (gene expression) layers. The backbone node level- and network level-perturbation amplitudes can be calculated by considering measured stimulus-vs-control gene expression changes (transcript) and the network topology (backbone layer) using a backward-causal reasoning algorithm. Three statistics are computed to assess the significance of a NPA score with respect to biological variation (confidence interval) and its specificity to the given two-layer network structure (*O* and *K* statistics). The NPA score computed for each network can be aggregated in a single value termed the BIF that quantifies the overall perturbation of the cellular system (Hoeng et al., 2014; Thomson et al., 2013). A collection of 57 subnetworks in 10 biological networks representative of main processes was used in our data analysis. All networks have been published and are accessible via http://causalbionet.com (Boue et al., 2015; sbv et al., 2013).

2.8.3. Pathway enrichment analysis of SRPs

Gene set enrichment analysis was conducted to identify biological pathways/processes associated with gene expression changes for each SRP. The mean of expression fold changes (as log 2) was calculated for each gene set (Ackermann and Strimmer 2009), and was used as the enrichment score. Gene resampling (Q1) was performed to generate the null hypothesis distribution and compute the significance associated with each gene set (Ackermann and Strimmer 2009). Hierarchical clustering of the enrichment score matrix (including gene sets with adjusted *p*-values below 0.01 in at least one SRP) was performed to group gene sets with similar enrichment score patterns across SRPs. The 1-correlation was used as a distance metric and the Ward method as an agglomerative algorithm.

2.9. Statistical analysis

Analysis of variance (ANOVA) followed by Dunnett's post-hoc test were performed to analyze statistical differences across treatment groups for functional endpoints (e.g., fold change of adhesion, and fold change of TNFα). Statistical analyses were performed on independent experiments, and in this context, data are presented as the mean ± standard error of the mean (SEM). Data from one experiment are reported as the mean ± standard deviation (SD) of replicate measurements and no statistics are shown (Cumming et al., 2007). R software version 3.1.2 was used for statistical analysis. Post-hoc tests were carried out using the "multcomp" R package (version 1.3-2). Statistical analysis of xMAP data was performed using SAS version 9.2. Values below either the least detectable dose (LDD) or the lower limit of quantification were replaced by the maximum of LDD or LLOQ. Descriptive statistics were then computed by group of interest and pairwise comparisons were performed using two-sample *t*-tests accounting for variance heterogeneity.

3. Results

This study aimed to compare the effects of aqueous extracts from the THS2.2 aerosol, a candidate MRTP, and 3R4F cigarette reference smoke on the adhesion of monocytic cells to primary human endothelial cells, a key step in the development of atherosclerosis. The approach combined functional measurements obtained using an in vitro adhesion assay with transcriptomics and inflammatory protein marker data to investigate cellular changes at the molecular levels in both MM6 cells and HCAECs.

3.1. Reduced carbonyl levels in the aqueous extract of the THS2.2 aerosol compared with that of 3R4F smoke at matched nicotine concentrations

The concentration of eight carbonyls was determined using LC-MS to monitor batch reproducibility of aqueous extractss from the THS2.2 aerosol and 3R4F smoke (Table 2). Average coefficients of

Table 2
Carbonyl and nicotine concentrations determination in THS2.2 and 3R4F aqueous extracts.

	3R4F sbPBS		THS2.2 abPBS		3R4F/THS2.2
Unit: μg/item	Mean	± SD	Mean	± SD	
Formaldehyde	42.0	6.4	**2.8**	0.9	15.2
Acetaldehyde	1168.4	155.0	**161.9**	23.7	7.1
Acetone	526.2	48.3	**29.4**	5.3	17.8
Acrolein	128.3	15.4	**7.0**	1.4	18.3
Propionaldehyde	59.1	18.2	**8.6**	2.9	6.9
Crotonaldehyde	57.8	7.9	**2.7**	0.6	21.4
Methyl ethyl ketone	127.6	17.1	**5.8**	1.2	21.9
Butyraldehyde	21.2	3.8	**8.6**	0.7	2.5
Nicotine	77.6	8.4	68.4	4.9	1.1

Analytes highligthed in bold showed significant differences (*t*-test; $p < 0.05$) between 3R4F and THS2.2. *N*, number of independent aqueous fractions generated. For carbonyl analysis, *N* = 34 and 16 for 3R4F and THS2.2, respectively. For nicotine, *N* = 5 for both.

variation of 16% and 21% were recorded for 3R4F and THS2.2 aqueous extracts, respectively. Carbonyl concentrations of the THS2.2 aqueous extract were significantly 2.5–22 times lower than those of 3R4F, whereas nicotine concentrations remained equivalent between both extracts (Table 2). The decreased amounts of carbonyls in the THS2.2 aqueous extract were consistent with lower yields per mg nicotine of 58 harmful and potentially harmful constituents (HPHC) measured in the THS2.2 aerosol compared with 3R4F smoke (Supplementary Table 1).

3.2. No significant increase of MM6 cell-HCAEC adhesion was observed following fresh direct and indirect exposures to THS2.2 aqueous extract at concentrations exhibiting maximal adhesion with 3R4F aqueous extract

Concentration–response experiments were conducted with THS2.2 and 3R4F aqueous extracts to identify the concentrations that exhibited the maximal MM6 cell-HCAEC adhesion rates or TNFα release by THS2.2 or 3R4F aqueous extract-treated MM6 cells (we have previously shown that TNFα, released from 3R4F aqueous extract (sbPBS)-treated MM6 cells, is one of the main driver of MM6 cell-HCAEC adhesion in indirect exposure conditions, (Poussin et al., 2015)) at low cell death rates (<25%) assessed using the resazurin assay (Supplementary information) or cell count (Supplementary Fig. 2). In the I treatment, the increase of 3R4F aqueous extract concentrations showed a biphasic response curve indicative of cytotoxic effects on MM6 cells beyond a certain concentration range (Supplementary Fig. 2A). A biphasic response curve was also observed with THS2.2 aqueous extract, however shifted towards 20–25-fold higher concentrations (Supplementary Fig. 2A ExpC). Similar results have been reported for THP-1 cells, another monocytic cell line, exposed to 3R4F smoke/THS2.2 aerosol-bubbled medium (van der Toorn et al., 2015a). In the FD treatment, the concentration-response curve for the adhesion rate displayed a S-shape and was accompanied by concentration-dependent loss of HCAECs due to cytotoxic effects of 3R4F aqueous extract with enhanced concentrations (Supplementary Fig. 2B). In concentration-response (Supplementary Fig. 2) and main experimental phases (Fig. 1 and Supplementary Fig. 3), 3R4F aqueous extract promoted maximum MM6 cell-HCAEC adhesion at low concentrations of 0.045–0.06 puffs/ml in the I treatment, and at a high concentration of 0.225 puffs/ml in the FD treatment. However, no significant increase in MM6 cell-HCAEC adhesion was observed when THS2.2 aqueous extract was used at the same concentrations as 3R4F in I and FD treatments. To achieve similar increases of MM6 cell-HCAEC adhesion with THS2.2 aqueous extract as observed for 3R4F, 10-fold higher concentrations (2.25 puffs/ml) were necessary for FD treatment, and 20–25-fold higher concentrations (1.125 puffs/ml) were required for I treatment (Fig. 1 and Supplementary Fig. 3). The highest concentrations of THS2.2 (2.25 puffs/ml) and 3R4F (0.225 puffs/ml) aqueous extracts used in the FD treatment induced a significant decrease (∼25%) in HCAEC numbers (Supplementary Fig. 2 and Poussin et al. (2015)). Moreover, no significant increase in MM6 cell-HCAEC adhesion was observed with 3R4F or THS2.2 in the D treatment at any concentration, except at 0.225 puffs/ml with 3R4F and 1.125 puffs/ml with THS2.2 which showed only a slight increase compared with same concentrations in the FD treatment. These differences observed between D and FD treatments could be explained by possible decay of unstable 3R4F smoke constituents during the preparation of unconditioned media used in the D treatment (Poussin et al., 2015). To mechanistically study the primary effects of 3R4F/THS2.2 aqueous extracts on HCAECs, endothelial cells were exposed to the different treatments for 4 h. Indeed, when activated, endothelial cells rapidly induce within 2–8 h the expression of adhesion molecules mediating leukocyte-endothelial cell adhesion (Scholz et al., 1996; Stocker et al., 2000). Longer exposure time could be further used to study secondary effects in vitro.

3.3. Reduced gene expression changes induced in HCAECs exposed to THS2.2 versus 3R4F

Transcriptomics profiling was performed on HCAECs following treatment for 4 h with conditioned media, unconditioned media or fresh aqueous extracts generated with THS2.2 aerosol or 3R4F smoke. Pairwise comparisons of gene expression levels measured for each concentration-treatment and respective vehicle controls were computed and corresponded to HCAEC SRPs.

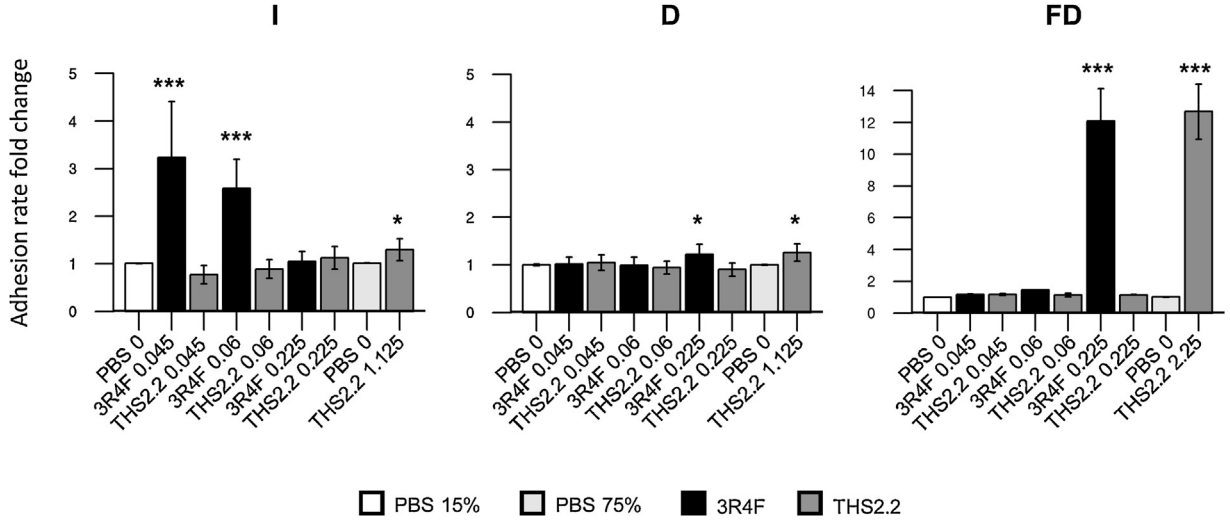


Fig. 1. Effects of THS2.2 and 3R4F aqueous extracts on the adhesion of MM6 cells to HCAECs following indirect (I), direct (D), and fresh direct (FD) treatments of HCAECs. Bar charts represent fold changes of the adhesion rate relative to respective vehicle controls. The adhesion rate reflects the number of adherent MM6 cells relative to the total number of HCAECs counted in the same well multiplied by 100. Data are presented as the mean ± SEM; $N = 2–3$ independent experiments ($n = 3–6$ replicates). $^{*}p \leq 0.05$, $^{***}p \leq 0.001$ vs. 0 puffs/ml (PBS 15% or 75%). THS2.2 or 3R4F aqueous extract concentrations are expressed in puffs/ml.

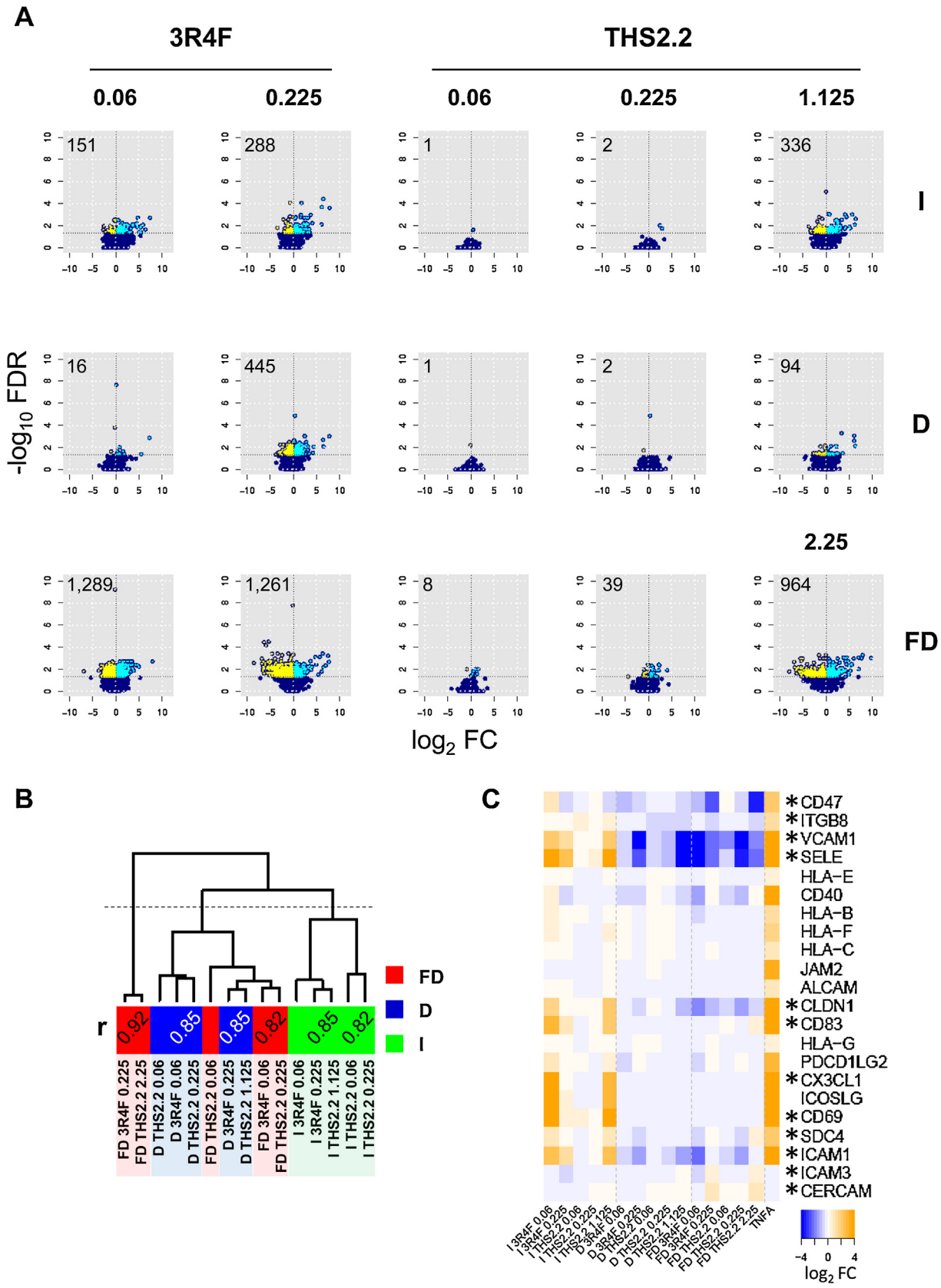


Fig. 2. Systems response profiles of HCAECs following indirect (I), direct (D) and fresh direct (FD) treatments with THS2.2 or 3R4F. (A) Volcano plots display gene expression change amplitude (as $\log_2$ fold-change) versus significance (as $-\log_{10}$ of adjusted *p*-value or false discovery rate) on the *x*- and *y*-axis, respectively. Significantly up (right)- and down (left)-regulated genes (FDR < 0.05) are highlighted in cyan and yellow, respectively. Total number of significantly regulated genes is indicated in the top–left corner of volcano plots. (B) Dendrogram showings hierarchical clustering of treatment group SRPs (distance: 1-correlation; agglomeration method: ward). Cutting the dendrogram at the depth indicated by the dotted line highlights three main clusters. r corresponds to the Pearson correlation coefficient ($p < 0.001$) between pairs of treatment group SRPs (detailed analysis in Supplementary Fig. 4). (C) Heatmap of expression fold-changes (FC; as $\log_2$ scale) across treatments of genes encoding adhesion molecules. *FDR < 0.05

The graphical representation of SRPs on volcano plots reveals a concentration-dependent increase in the magnitude and statistical significance of gene expression fold-changes in all 3R4F treatments, leading to an increased numbers of DEGs (Fig. 2A). At the same concentrations, only a few genes reached statistical significance following THS2.2 exposure. When the concentrations of THS2.2 aqueous extract were increased by 10 and 20 fold for I and FD treatments, respectively, similar numbers of DEGs, were obtained. Maximum numbers of DEGs were obtained with 3R4F and THS2.2 FD treatments (Fig. 2A).

Hierarchical clustering based on gene expression fold-changes revealed three main cliques that grouped all SRPs for the I treatment in one cluster, SRPs obtained with the highest concentrations of THS2.2 (2.25 puffs/ml) and 3R4F (0.225 puffs/ml) aqueous extracts for the FD treatment in a second cluster, and the remaining SRPs for the D and FD treatments in the third cluster (Fig. 2B). The calculation of pairwise gene expression fold-change (restricted to genes with significant changes in at least one SRP) correlation coefficients enabled us to identify SRPs with the most similar gene expression changes. Indeed, changes observed at intermediate concentrations of THS2.2 (0.225 puffs/ml) were generally similar to those observed at a low concentration of 3R4F (0.06 puffs/ml), while changes observed at the highest concentration of THS2.2 (1.125 or 2.25 puffs/ml) resembled those measured at the highest concentration of 3R4F (0.225 puffs/ml) (Fig. 2B and Supplementary Fig. 4). We investigated genes that showed significant expression changes induced by THS2.2, but not by 3R4F (Supplementary Table 2). In most cases, the directionality and magnitude of expression changes of these genes were comparable between THS2.2 and 3R4F treatments. However, their FDR values (adjusted P-values) did not reach significance for 3R4F probably because of higher within-group variability. Few genes showed different patterns of expression changes between THS2.2 and 3R4F (Supplementary Table 2).

To relate the functional adhesion results with molecular changes in HCAECs, we investigated the expression changes of genes encoding adhesion molecules (Fig. 2C). Significant increases in the mRNA expression of most adhesion molecules were detected only following the I treatment at the low concentration of 3R4F aqueous extract (0.06 puffs/ml) and the high concentration of THS2.2 aqueous extract (1.125 puffs/ml), and to a lower extent at the high concentration of 3R4F aqueous extract (0.225 puffs/ml). After the D and FD treatments, no significant regulation or even down-regulation of gene expression was observed, with the exception of Cerebral Endothelial Cell Adhesion Molecule (CERCAM) and Intercellular Adhesion Molecule 3 (ICAM-3) genes, which tended to show up-regulation only with the highest concentrations of 3R4F and THS2.2 aqueous extracts after the FD treatment (Fig. 2C).

3.4. Reduced network perturbation amplitudes and biological impact factors computed from the systems response profiles of HCAECs exposed to THS2.2 as compared with 3R4F

A computational systems biology approach based on transcriptomics data with two-layer cause-and-effect network models was used to conduct NPA analysis and quantify the overall biological impact of THS2.2 compared with 3R4F after I, D and FD treatments. This analysis included a collection of 57 published biological networks/subnetworks that model processes of proliferation and senescence, cell stress, vascular inflammation, DNA damage, cell death (apoptosis and necroptosis), and autophagy (Supplementary Table 3). The NPA scores calculated for each SRP (Supplementary Fig. 5) and network/subnetwork were then aggregated as a single BIF value that quantifies the overall perturbation of the system. The maximum biological impact, set to 100% and used as a reference, was obtained for I 3R4F 0.06 showing a broad spectrum of perturbed networks (Fig. 3A). A comparable pattern of networks was perturbed at a higher concentration of 3R4F aqueous extract (0.225 puffs/ml) with similar underlying perturbed biology ($\delta = 0.91$), but with a lower amplitude (relative biological impact factor (RBIF) = 60%). At the same concentrations (0.06 and 0.225 puffs/ml), the overall magnitude of perturbation promoted by THS2.2 aqueous extract represented only 1% and 3% of the total perturbation of the reference, respectively, while this was 78% at the highest concentration with highly similar perturbed biology ($\delta = 0.96$) (Fig. 3A). The pattern and magnitude of perturbed networks for the D and FD treatments differed from those of the I treatment. However, similar to the I treatment, the biological impacts of THS2.2 in HCAECs represented 1% and 3% for the D treatment as well as 1% and 8% for the FD treatment at low and intermediate concentrations, respectively (Fig. 3A). At high concentrations of THS2.2 aqueous extract, the RBIF corresponded to 31% and 36% of the total perturbation of the reference for D and FD treatments, respectively (Fig. 3A).

Principal component analysis of the SRP matrix (fold-change matrix) emphasized that the separation of I, D/FD and high concentration FD treatments in sub-space directions maximizing data variance was driven by genes that have roles in inflammatory and cell stress responses (data not shown, see Poussin et al. (2015)). Therefore, the activated Vascular-Inflammatory Processes network (V-IPN) and the Cell Stress network were investigated in more detail. Significant perturbations of the V-IPN/endothelial cell–monocyte interaction subnetwork were only observed in the I treatment, at a high concentration for THS2.2 aqueous extract (1.125 puffs/ml), but at low (0.06 puffs/ml) and high (0.225 puffs/ml) concentrations for 3R4F aqueous extract (Fig. 3B). The NPA and backbone score contributions (Supplementary Table 4) for most nodes showed comparable patterns across concentration/treatment groups to that obtained for the functional adhesion results (Fig. 1). Regarding the Cell Stress network, the Xenobiotic Metabolism Response subnetwork was perturbed in a concentration-dependent manner with considerably lower amplitudes at low (0.06 puffs/ml) and intermediate (0.225 puffs/ml) concentrations of THS2.2 aqueous extracts when compared with 3R4F. At the highest concentrations of the FD treatment, the nature of the stress responses differed compared with D and I treatments. The Endoplasmic Reticulum Stress subnetwork and the Oxidative Stress subnetwork were significantly and similarly perturbed in both I and FD treatments (at high concentrations only); however they displayed different pattern of leading nodes, indicative of different underlying perturbed biology (Fig. 3B and Supplementary Table 4). Indeed, the nodes that contributed the most to the NPA score for the I treatment and little for the FD treatment were “Particulate Matter”, “Reactive Oxygen Species”, “kaof(p38 MAPK family Hs)”, “taof(NFKB Complex Hs)”, “NFKB Complex Hs” and “Glutathione”. For the FD treatment, specific node contributors included kaof(MAPK8) and MAPK8 (Supplementary Table 4).

As a complementary computational approach to identify regulated biological processes/pathways in HCAECs, enrichment analysis was conducted using each SRP. The clustering of the gene set enrichment score matrix revealed different patterns of regulated biological processes (Fig. 4). The heatmap including

for at least one SRP (not considering TNFα SRP, here). THS2.2 or 3R4F aqueous extract concentrations are expressed in puffs/ml. (For interpretation of the references to color in this figure legend, the reader is referred to the web version of this article.)

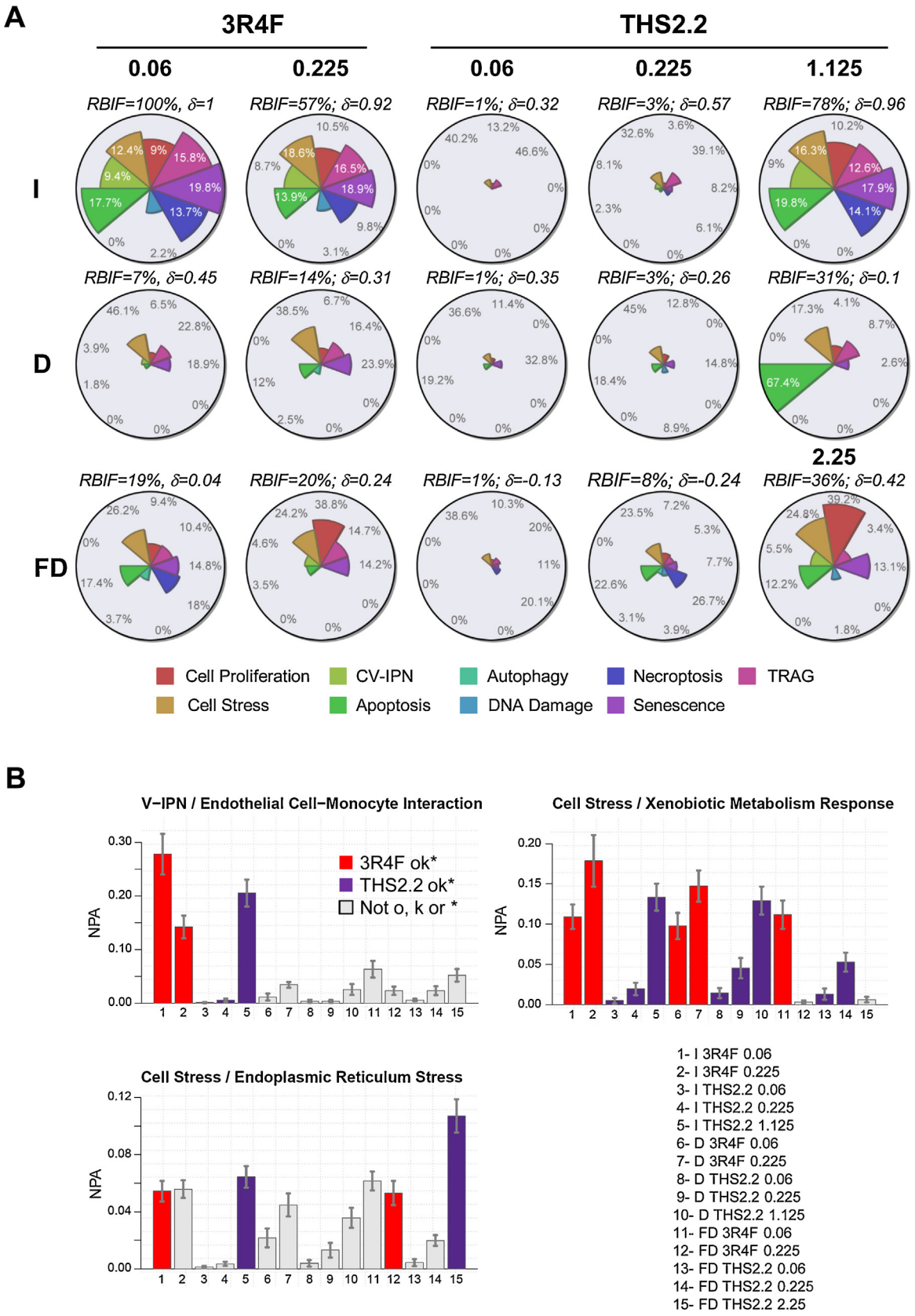


Fig. 3. Computated biological impact factors and network perturbation amplitudes in HCAECs following indirect (I), direct (D) and fresh direct (FD) treatments with THS2.2 or 3R4F. (A) The NPA computed for each network leveraging transcriptomics data was aggregated as a single value termed the biological impact factor (BIF) that quantifies the overall perturbation of the system modeled in causal networks. For each SRP, the contribution of significantly perturbed biological networks to the overall BIF is represented by colored surfaces proportionally covering circular plots and indicated as a percentage. These colored surfaces are also comparable across SRPs. The BIF associated with the SRP that induces the maximum network perturbation was automatically set to 100% as the reference (relative (R)BIFref). RBIF related to other SRPs was expressed as a percentage of the RBIFref. The delta (d, [−1,1]) value reflects the degree to which the underlying biology modeled in the networks is similarly perturbed compared with the

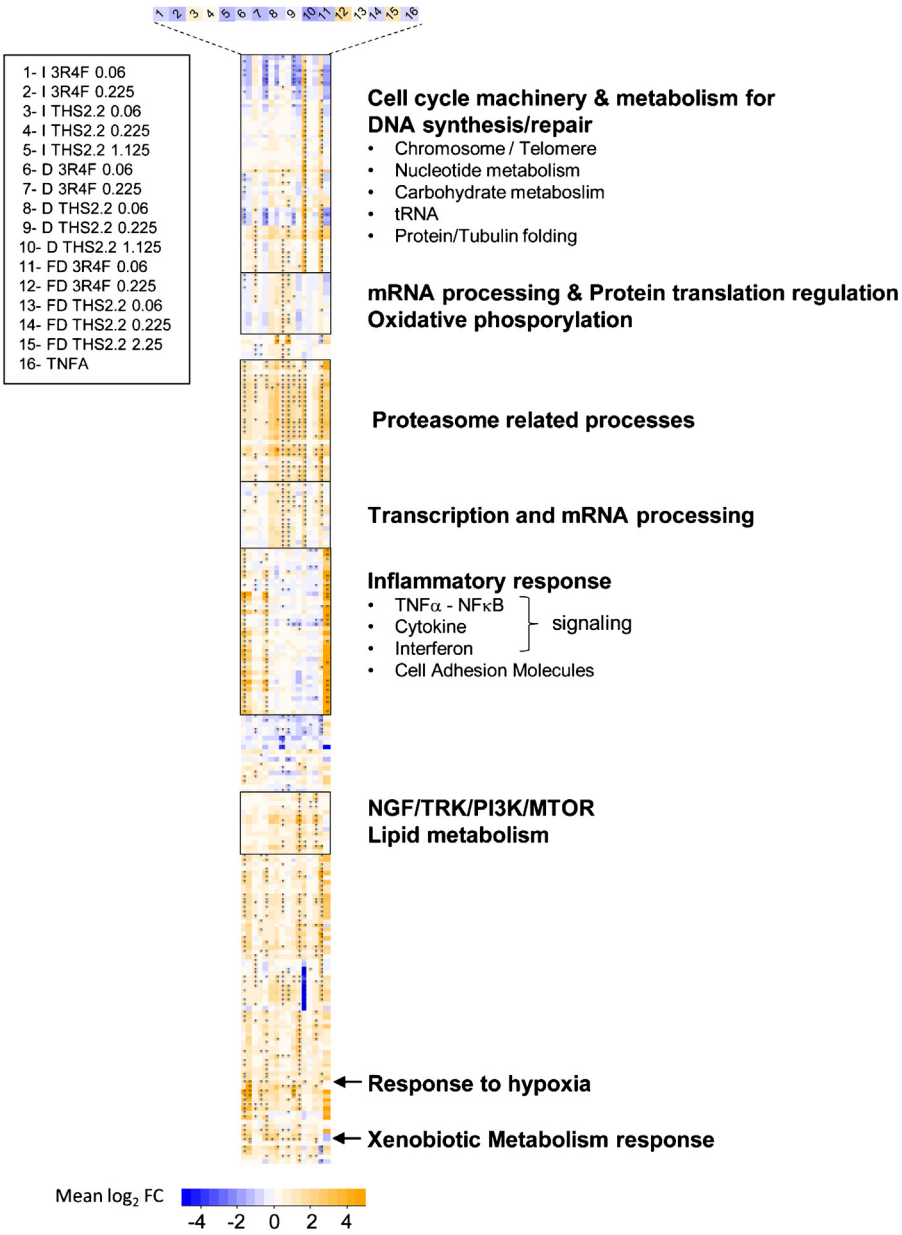


Fig. 4. Gene set enrichment analysis of HCAEC systems response profiles. Heatmap of enrichment scores corresponding to mean of gene expression fold-changes for each gene set (MSigDB C2CP collection) and an adjusted p-value <0.01 in at least one concentration-treatment condition. * adjusted p-value <0.05. The heatmap with all gene set names is shown in Supplementary Fig. 6.

all gene set names are shown in Supplementary Fig. 6. Consistent with the observation of significant perturbations of the Proliferation Network, and more particularly the Cell Cycle subnetwork at high concentrations of 3R4F (0.225 puffs/ml) and THS2.2 (2.25 puffs/ml) aqueous extracts (Fig. 3A and Supplementary Fig. 5), the enrichment analysis identified gene sets involved in cell cycle machinery and DNA synthesis and repair under those same conditions (Fig. 4 and Supplementary Fig. 6). Enriched gene sets representative of an inflammatory response such as TNF-, cytokine signaling-, NFκB-, cell adhesion molecules-related gene sets, showed averaged concentration-dependent increases with I treatment (3R4F, 0.06 and 0.225 puff/ml; THS2.2, 1.125 puffs/ml) and no regulation or even concentration-dependent decreases in D and FD treatments (Fig. 4 and Supplementary Fig. 6). These results were consistent with the perturbation pattern of the V-IPN/endothelial cell–monocyte interaction subnetwork which models the mechanism of monocyte–endothelial cell adhesion mediated by vascular inflammation (Fig. 3B). Enrichment and NPA results were also in agreement for the process of xenobiotic metabolism response (Figs. Fig. 3B and Fig. 4 and Supplementary Fig. 6).

reference SRP. (B) Bar charts show NPA scores for three sub-networks of interest. The NPA is considered to be significant when both O and K statistics reach significance at the 0.05 level as indicated by o and k, respectively, when the significance with respect to the experimental variation is below a threshold p-value of 0.05 (*). Error bars represent the 95% confidence interval. THS2.2 or 3R4F aqueous extract concentrations are expressed in puffs/ml. Abbreviations: V-IPN, vascular-inflammatory processes network; TRAG, tissue repair and angiogenesis network.

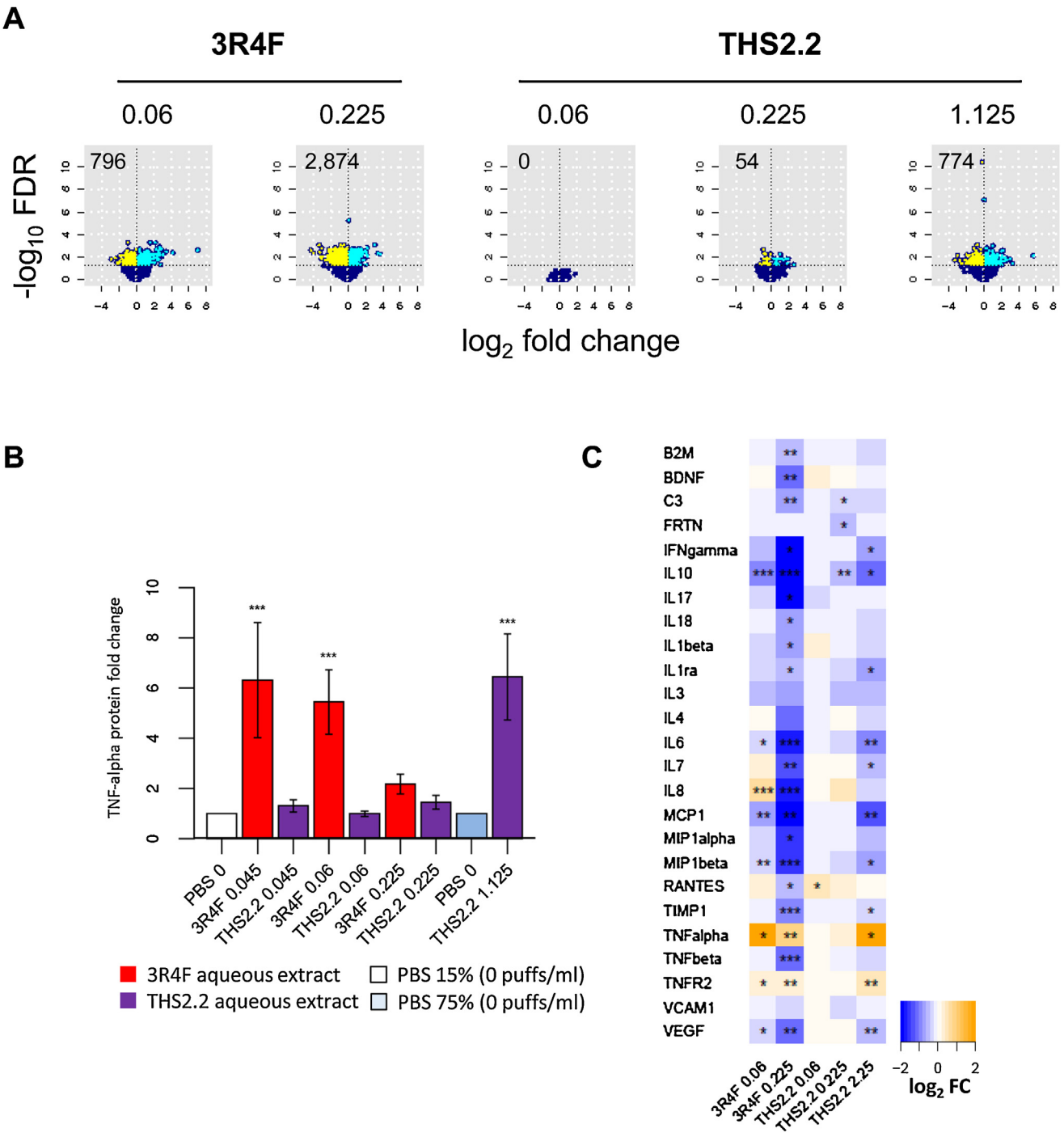


Fig. 5. Systems response profiles of MM6 cells and inflammatory protein markers released in conditioned media following exposure to freshly generated THS2.2 or 3R4F aqueous extracts. (A) Volcano plots display gene expression change amplitudes (as $\log_2$ fold change) versus significance (as $-\log_{10}$ of adjusted *p*-value or false discovery rate) on the *x*- and *y*-axis, respectively. Significantly up- (right) and down (left)-regulated genes (FDR < 0.05) are highlighted in cyan and yellow, respectively. (B) Relative TNFα levels measured in conditioned media (MM6 cell supernatants) by ELISA, and expressed as fold change relative to the vehicle controls. (C) Heatmap of inflammatory markers quantified in conditioned media (fold change values of treatment group versus their respective vehicle control). $^{*}p \leq 0.05$, $^{**}p \leq 0.01$, $^{***}p \leq 0.001$ (unadjusted *p*-values are reported). THS2.2 or 3R4F aqueous extract concentrations are expressed in puffs/ml. (For interpretation of the references to color in this figure legend, the reader is referred to the web version of this article.)

Additional gene sets representative of processes such as mRNA processing and protein translation regulation, ubiquitin-proteasome-related processes, oxidative phosphorylation, lipid metabolism, MAP kinase signaling, and growth factor signaling were found to be significantly enriched following different patterns across SRPs (Fig. 4 and Supplementary Fig. 6).

3.5. Lower effects of THS2.2 versus 3R4F aqueous extracts on gene expression changes in MM6 cells and on the release of inflammatory marker proteins in conditioned media.

A concentration-dependent increase of DEGs in MM6 cells was observed in response to both THS2.2 and 3R4F aqueous extracts

after 2 h exposure. At low (0.06 puffs/ml) and intermediate (0.225 puffs/ml) concentrations of THS2.2 aqueous extract, no and 54 DEGs were counted, respectively, while those numbers increased to 796 and 2874, respectively for 3R4F aqueous extract (Fig. 5A). A 20-fold higher concentration of THS2.2 aqueous extract (1.125 puffs/ml) led to similar number of DEGs compared with that observed for the low 3R4F aqueous extract concentration (Fig. 5A). Pairwise correlation analysis of MM6 cell SRPs showed the highest fold-change similarities between THS2.2 0.225 and 3R4F 0.06 ($r = 0.80$), and between THS2.2 1.125 and 3R4F 0.225 ($r = 0.78$) (Supplementary Fig. 7). When analyzing genes that reached statistical significance for regulation by THS2.2 aqueous extract (207 genes), but not 3R4F aqueous extract, most showed similar levels and directionalities of expression change to those regulated by 3R4F aqueous extract (Supplementary Table 5). Among those 207 unique genes, only three showed a different directionality of regulation compared with those observed in response to 3R4F, but with smaller fold-changes (gene names highlighted in yellow in the Supplementary Table 5). Of note, MM6 cell viability decreased by ~20-25% at the highest concentrations for both 3R4F (0.225 puffs/ml) and THS2.2 (1.125 puffs/ml) aqueous extracts, suggesting the induction of cytotoxic effects (Supplementary Fig. 2 and data not shown).

The levels of inflammatory marker proteins measured in conditioned media revealed a concentration-dependent release of soluble mediators, with increased release of TNFα, TNF receptor 2, and interleukin (IL)-8 at low 3R4F aqueous extract concentrations only, but a decreased production for the other mediators (Fig. 5B and C; Supplementary Table 6). At low (0.06 puffs/ml) and intermediate (0.225 puffs/ml) concentrations, THS2.2 aqueous extract had restricted effects, while at a high concentration, the pattern of mediator release was intermediate between that observed for 3R4F at low and high concentrations (Fig. 5C and Supplementary Table 6). Analytes with measurements below the lower limit of quantification were excluded from the analysis.

3.6. Reduced network perturbation amplitudes and biological impact factors computed from the systems response profiles of MM6 cells exposed to THS2.2 aqueous extract as compared with 3R4F

A collection of 54 subnetworks belonging to nine main networks was used for NPA and BIF analysis of MM6 cell SRPs (Supplementary Table 3). As observed with HCAECs, the largest biological impact was promoted by a low concentration of 3R4F aqueous extract (0.06 puffs/ml). At the highest concentration of 3R4F aqueous extract (0.225 puffs/ml) the RBIF was 17% and the delta value was 0.1, indicating a low similarity regarding underlying perturbed biology compared with the low 3R4F aqueous extract concentration. The network perturbations observed with THS2.2 showed consistent concentration-dependent inflation leading to a RBIF of 34% and a delta value of 0.52 (Fig. 6). NPA scores associated with MM6 cell SRPs for each subnetwork are shown in Supplementary Fig. 8. Concentration-dependent increase of enrichment scores were also observed when conducting enrichment analysis using gene sets representative of canonical pathways/processes (Fig. 7 and Supplementary Fig. 9). Many gene sets involved in cell cycle/proliferation were found to be down-regulated in a consistent manner with leading nodes of significantly perturbed Cell Cycle subnetwork (e.g., leading nodes such as “taof(E2F1)”, “taof(E2F2)”, “taof(E2F3)”, “cell proliferation” were down-regulated, whereas “ATM”, “taof(E2F4)”, “CDKN1A”, “RB1” were up-regulated, data not shown) possibly indicative of MM6 cell cycle arrest (Supplementary Fig. 9). By contrast, gene sets such as oxidative stress and xenobiotic metabolism were up-regulated at low and intermediate concentrations of 3R4F and THS2.2 aqueous extracts, respectively. At the highest concentrations, the up-regulation of these gene sets was reduced. Of note, gene sets related to fatty acid, steroid and arachidonic metabolism showed a similar up-regulated pattern but the maximum enrichment score was obtained at the lowest 3R4F aqueous extract concentration for the two latter pathways. mRNA expression changes of prostaglandin-endoperoxide synthase 2 (PTGS2) which converts arachidonic

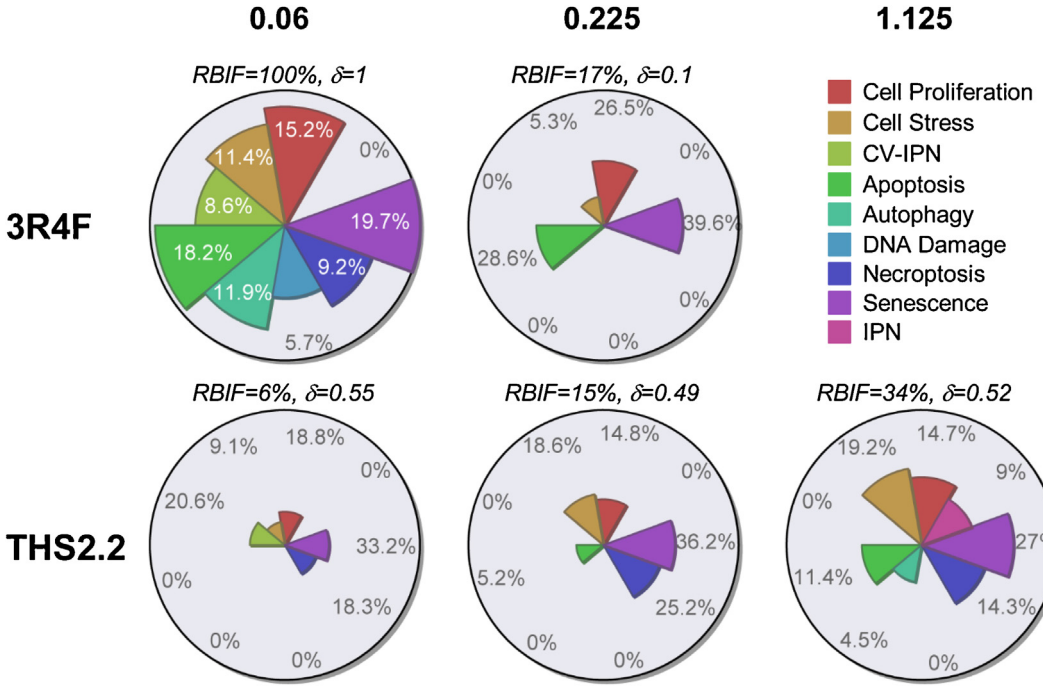


Fig. 6. Computed biological impact factors and network perturbation amplitudes in MM6 cells following exposure to THS2.2 or 3R4F aqueous extracts (see legend details in Fig. 3). THS2.2 or 3R4F aqueous extract concentrations are expressed in puffs/ml.

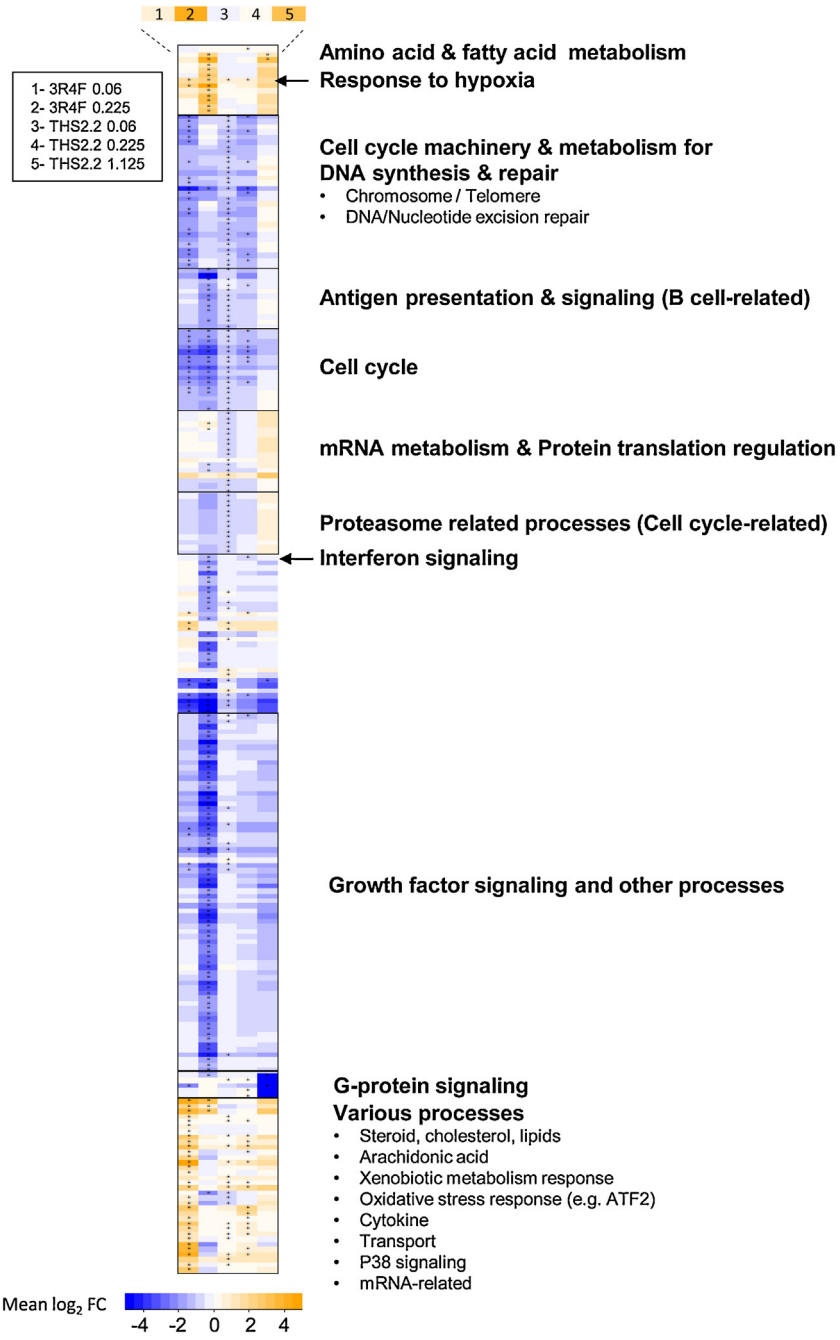


Fig. 7. Gene set enrichment analysis of MM6 systems response profiles. Heatmap of enrichment scores corresponding to mean of gene expression fold-changes for each gene set (MSigDB C2CP collection) and an adjusted p-value <0.01 in at least one concentration-treatment condition. * adjusted p-value <0.05. The heatmap with all gene set names is shown in Supplementary Fig. 9.

acid to prostaglandin H2, also followed a similar pattern (data not shown). When activated, the arachidonic acid pathway can lead to the production of lipids such as prostaglandins, which are implicated in inflammatory processes. Consistent with gene set enrichment, the PGE2 subnetwork was significantly perturbed at low concentrations of 3R4F aqueous extract and showed reduced perturbation at high concentrations, while concentration-dependent increase in perturbation were observed with THS2.2 aqueous extract, without reaching significance (Supplementary Fig. 8).

4. Discussion

The present work assessed the biological impact of THS2.2, a candidate MRTP, compared with that of a reference cigarette on the adhesion of monocytic cells to primary endothelial cells in vitro using a previously established experimental and computational systems biology/toxicology analysis framework (Poussin et al., 2015). The indirect and direct treatment of HCAECs with low and high concentrations of aqueous smoke/aerosol extracts via

different exposure modalities enabled us to differentiate the effects of stable and unstable smoke/aerosol constituents alone or in combination with MM6-derived soluble mediators present in conditioned media.

Previous in-depth investigations of the effects of aqueous 3R4F smoke extract revealed significant increases of MM6 cell-HCAEC adhesion mediated by distinct mechanisms in I and FD treatments of HCAECs, but not in the D treatment, at low and high concentrations, respectively. Following the I treatment, soluble mediators released by monocytic cells exposed to low concentrations of 3R4F aqueous extract activated a nuclear factor κB-mediated inflammatory response in HCAECs via a paracrine effect leading to a significant increase of adhesion proteins such as E-Selectin, ICAM-1, and subsequent MM6 cell–HCAEC adhesion. TNFα, identified as a key driver of this process, was shed from MM6 cell membranes following TACE activation by unstable 3R4F smoke constituents (Poussin et al., 2015). Following the FD treatment, a high concentration of unstable or a combination of stable and unstable 3R4F smoke constituents, triggered an augmentation of MM6 cell–HCAEC adhesion. This adhesion was associated with cytotoxic effects, leading to irreversible cellular damages and loss. Although stable 3R4F smoke constituents alone had limited effect on the adhesion of MM6 cells to HCAECs after 4 h, they elicited a cell stress response (e.g., concentration-dependent xenobiotic metabolism response) of a different nature than that caused by the combination of stable and unstable CS constituents (e.g., endoplasmic reticulum stress response) (Poussin et al., 2015). All these mechanistic insights have been extensively discussed in the context of the literature in Poussin et al' paper, and are leveraged for interpretation and discussion of the current work focusing on the comparison of the biological effects of THS2.2 with that of a reference cigarette.

At the same concentrations tested for 3R4F aqueous extract, THS2.2 aqueous extract in the present study did not promote significant MM6 cell-HCAEC adhesion and induced few gene expression changes in HCAECs following I, D or FD treatments. This resulted in low level or even no significant perturbation of biological processes modeled by networks or represented by gene sets. Indeed, 10- and 20-fold increases of THS2.2 aqueous extract concentrations were necessary to observe augmentations of MM6 cell-HCAEC adhesion similar to levels measured with 3R4F in both FD and I treatments, respectively. Comparisons at the gene expression or processes/networks levels of molecular changes in HCAECs overall showed important similarities between the highest concentrations of THS2.2 and the lowest or highest concentrations of 3R4F suggesting that similar biological pathways had been perturbed. A small subset of genes was found to have a different pattern of regulation in HCAECs and MM6 cells induced by the high concentration of THS2.2 compared with 3R4F. Further investigations will be needed to understand whether these differences reflect more granular concentration-dependent effects or other biological processes.

Our findings at the molecular level were consistent with the functional response that showed a shift of the concentration-response curve towards higher concentrations of THS2.2 aqueous extract necessary for the induction of MM6 cell-HCAEC adhesion seen with 3R4F. This curve shift may be explained by the lower levels of active aerosol-derived constituents present in the aqueous extract generated with THS2.2 compared with 3R4F, as reflected by the concentrations of some carbonyls, for matching nicotine levels. THS2.2 is based on a technology that heats tobacco instead of burning it. By not burning (i.e., combusting) the tobacco the extent of pyrolysis and the amount of combusted products is therefore lowered in the aerosol (Schorp et al., 2012; Werley et al., 2008). Mass spectrometry chemical characterization of the THS2.2 aerosol clearly showed a decreased complexity of the chemical mixture and a significant reduction of levels compared with an equivalent nicotine concentration of 3R4F smoke as measured in mass spectra, and also more specifically quantified for 58 constituents (Supplementary Table 1) derived from a list of 93 chemicals identified by the US Food and Drug Administration as HPHCs in tobacco products and tobacco smoke (Administration, 2012). Thus, this observation and previous studies of MRTPs suggest that a reduced exposure of biological systems to potentially harmful smoke constituents may translate to reduced damage to cells, tissues and organs when exposed to aerosol or aerosol fractions (Kogel et al., 2014; Phillips et al., 2015a; van der Toorn et al., 2015b). Our in vitro results are also consistent with and strengthened by the observations of significantly reduced effects of THS2.2 aqueous extract on chemotaxis and transendothelial migration compared with 3R4F (van der Toorn et al. 2015a) as well as reduced atherosclerotic plaque formation in ApoE$^{-/-}$ mice (prone to atherosclerosis) exposed to THS2.2 for 8 months compared with 3R4F (Phillips et al., 2015b).

Our results suggest that the distinct mechanisms leading to MM6 cell-HCAEC adhesion promoted by THS2.2 only at high concentrations of aqueous extract in FD and I treatments are similar to those described for the 3R4F aqueous extract at lower concentrations. Additionally, the inflammatory protein marker profile of supernatants collected after exposure of MM6 cells to high THS2.2 aqueous extract concentrations was comparable to the profile obtained for low 3R4F aqueous extract concentration, and showed an increase of TNFα secretion, a key inducer of MM6 cell–endothelial cell adhesion (Poussin et al. 2014, 2015). In line with our results, the increase of TNFα or other cytokine/chemokine mRNA expression or protein release promoted by CS have been previously reported in monocytic cells, macrophages or human primary peripheral blood monocytes (Demirjian et al. 2006; van Leeuwen et al. 2005; Wright et al. 2012). The shift of the concentration-response to the right was consistent with another study showing a shift towards high concentrations of the concentration-response curves for the release of TNFα and IL-8 by monocytic THP-1 cells exposed to a pMRTP or THS2.2 compared with a reference cigarette (van der Toorn et al. 2015a, 2015b). Moreover, these publications reported reduced effects of both heat-not-burn tobacco products on chemotaxis and transendothelial migration of monocytes which are important vascular processes that when deregulated concomitantly with endothelial adhesive properties contribute to the development of atherosclerosis (van der Toorn et al. 2015a, 2015b).

5. Conclusions

In summary, our results show that 3R4F smoke in the form of an aqueous extract promoted the adhesion of monocytic cells to endothelial cells via distinct indirect and direct CS-induced concentration-dependent mechanisms. At matching concentrations with equivalent nicotine levels, the THS2.2 aqueous extract did not trigger MM6 cell-HCAEC adhesion, and clearly showed reduced impact at molecular levels in HCAECs and MM6 cells. MM6 cell-HCAEC adhesion accompanied by molecular changes in both cell types only reached similar levels of increase to those induced by 3R4F aqueous smoke extract when concentrations of THS2.2 aqueous extract were raised by 10- and 20-fold for FD and I exposure modalities, respectively. Comparisons at gene and biological network/pathway levels demonstrated strong similarities in molecular changes induced by high THS2.2 aqueous extract concentrations compared with low 3R4F aqueous extract concentrations in both cell types indicating that the THS2.2 aqueous extract promoted adhesion of monocytic cells to endothelial cells via similar indirect and direct mechanisms to those described for 3R4F aqueous extract. These data, along with ones cited, indicate

the potential of a heat-not-burn tobacco product to reduce the risk for cardiovascular disease compared to combustible cigarettes.

Funding

This work was funded by Philip Morris International R&D.

Acknowledgements

We would like to thank Didier Goedertier and Claudius Pak for generating fresh aqueous smoke/aerosol extracts for each experiment; Karine Baumer and Dariusz Peric for mRNA extraction; Emmanuel Guedj and Rémi Dulize for generating transcriptomics data; Dr Nikolai Ivanov for providing laboratory resources for the generation of transcriptomics data; Dr Grégory Vuillaume for the statistical analysis of xMAP data; Dr Sam Ansari for submitting transcriptomics data to the Array Express repository database; The Aerosol Chemistry Analytical Laboratory and Quentin Dutertre for carbonyl and nicotine concentration determination, respectively; Dr Stefan Frentzel for generous support of laboratory resources for the experimental work; Drs Walter Schlage and Filippo Zanetti for scientific review of the manuscript. This work was funded by Philip Morris International R&D.

Appendix A. Supplementary data

Supplementary data associated with this article can be found, in the online version, at http://dx.doi.org/10.1016/j.tox.2015.11.007.

References

Ackermann, M., Strimmer, K., 2009. A general modular framework for gene set enrichment analysis. BMC Bioinf. 10, 47.

Benjamini, Y., Hochberg, Y., 1995. Controlling the false discovery rate: a practical and powerful approach to multiple testing. J. R. Stat. Soc. Ser. B 57, 289–300.

Boue, S., Talikka, M., Westra, J.W., Hayes, W., Di Fabio, A., Park, J., Schlage, W.K., Sewer, A., Fields, B., Ansari, S., Martin, F., Veljkovic, E., Kenney, R., Peitsch, M.C., Hoeng, J., 2015. Causal biological network database: a comprehensive platform of causal biological network models focused on the pulmonary and vascular systems. Database 2015, bav030.

Cumming, G., Fidler, F., Vaux, D.L., 2007. Error bars in experimental biology. J. Cell Biol. 177, 7–11.

Demirjian, L., Abboud, R.T., Li, H., Duronio, V., 2006. Acute effect of cigarette smoke on TNF-alpha release by macrophages mediated through the erk1/2 pathway. Biochim. Biophys. Acta 1762, 592–597.

Favero, G., Paganelli, C., Buffoli, B., Rodella, L.F., Rezzani, R., 2014. Endothelium and its alterations in cardiovascular diseases: life style intervention. BioMed Res. Int. 2014 (801896) .

Food and Drug Administration, 2012. Harmful and Potentially Harmful Constituents in Tobacco Products and Tobacco Smoke; Established List. U.S. Department of Health and Human Services, Food and Drug Administration, Rockville, MD: Center for Tobacco Products. In Federal Register 77, 20034–20037.

Food and Drug Administration, 2012. Modified Risk Tobacco Product Applications: Draft Guidance for Industry.

Haussmann, H.J., 2012. Use of hazard indices for a theoretical evaluation of cigarette smoke composition. Chem. Res. Toxicol. 25, 794–810.

Hermida, L., Poussin, C., Stadler, M.B., Gubian, S., Sewer, A., Gaidatzis, D., Hotz, H.R., Martin, F., Belcastro, V., Cano, S., Peitsch, M.C., Hoeng, J., 2013. Confero: an integrated contrast data and gene set platform for computational analysis and biological interpretation of omics data. BMC Genomics 14, 514.

Hoeng, J., Talikka, M., Martin, F., Sewer, A., Yang, X., Iskandar, A., Schlage, W.K., Peitsch, M.C., 2014. Case study: the role of mechanistic network models in systems toxicology. Drug Discov. Today 19, 183–192.

Kalra, V.K., Ying, Y., Deemer, K., Natarajan, R., Nadler, J.L., Coates, T.D., 1994. Mechanism of cigarette smoke condensate induced adhesion of human monocytes to cultured endothelial cells. J. Cell. Physiol. 160, 154–162.

Kogel, U., Schlage, W.K., Martin, F., Xiang, Y., Ansari, S., Leroy, P., Vanscheeuwijck, P., Gebel, S., Buettner, A., Wyss, C., Esposito, M., Hoeng, J., Peitsch, M.C., 2014. A 28-day rat inhalation study with an integrated molecular toxicology endpoint demonstrates reduced exposure effects for a prototypic modified risk tobacco product compared with conventional cigarettes. Food Chem. Toxicol. 68, 204–217.

Lehr, H.A., 1993. Adhesion-promoting effects of cigarette smoke on leukocytes and endothelial cells. Ann. N. Y. Acad. Sci. 686, 112–118 discussion 118–119.

Martin, F., Sewer, A., Talikka, M., Xiang, Y., Hoeng, J., Peitsch, M.C., 2014. Quantification of biological network perturbations for mechanistic insight and diagnostics using two-layer causal models. BMC Bioinf. 15, 238.

Messner, B., Bernhard, D., 2014. Smoking and cardiovascular disease: mechanisms of endothelial dysfunction and early atherogenesis. Arterioscler. Thromb. Vasc. Biol. 34, 509–515.

Perfetti, T.A., Rodgman, A., 2011. The complexity of tobacco and tobacco smoke. Beitrage zur Tabakforschung International 24, 215–232.

Phillips, B., Veljkovic, E., Peck, M.J., Buettner, A., Elamin, A., Guedj, E., Vuillaume, G., Ivanov, N.V., Martin, F., Boue, S., Schlage, W.K., Schneider, T., Titz, B., Talikka, M., Vanscheeuwijck, P., Hoeng, J., Peitsch, M.C., 2015a. A 7-month cigarette smoke inhalation study in C57BL/6 mice demonstrates reduced lung inflammation and emphysema following smoking cessation or aerosol exposure from a prototypic modified risk tobacco product. Food Chemical Toxicol. 80, 328–345.

Phillips, B., Veljkovic, E., Boue, S., Schlage, W.K., Vuillaume, G., Martin, F., Titz, B., Leroy, P., Buettner, A., Elamin, A., Oviedo, A., Cabanski, M., Guedj, E., Schneider, T., Talikka, M., Ivanov, N.V., Vanscheeuwijck, P., Peitsch, M.C., Hoeng, J., 2015b. An 8-month systems toxicology inhalation/cessation study in apoe-/- mice to investigate cardiovascular and respiratory exposure effects of a candidate modified risk tobacco product, THS 2.2, compared with conventional cigarettes. Toxicol. Sci. doi:http://dx.doi.org/10.1093/toxsci/kfv243.

Poussin, C., Gallitz, I., Schlage, W.K., Steffen, Y., Stolle, K., Lebrun, S., Hoeng, J., Peitsch, M.C., Lietz, M., 2014. Mechanism of an indirect effect of aqueous cigarette smoke extract on the adhesion of monocytic cells to endothelial cells in an in vitro assay revealed by transcriptomics analysis. Toxicol. in Vitro 28, 896–908.

Poussin, C., Laurent, A., Peitsch, M.C., Hoeng, J., De Leon, H., 2015. Systems biology reveals cigarette smoke-induced concentration-dependent direct and indirect mechanisms that promote monocyte-endothelial cell adhesion. Toxicol. Sci. 147, 370–385.

Rodgman, A., Perfetti, T.A., 2013. The Chemical Components of Tobacco and Tobacco Smoke, Second ed. CRC Press.

sbv IMPROVER project team, Ansari, S., Binder, J., Boue, S., Di Fabio, A., Hayes, W., Hoeng, J., Iskandar, A., Kleiman, R., Norel, R., O'Neel, B., Peitsch, M.C., Poussin, C., Pratt, D., Rhrissorrakrai, K., Schlage, W.K., Stolovitzky, G., Talikka, M., 2013. On Crowd-verification of Biological Networks. Bioinfor. Biol. Insights 7, 307–325.

Scholz, D., Devaux, B., Hirche, A., Potzsch, B., Kropp, B., Schaper, W., Schaper, J., 1996. Expression of adhesion molecules is specific and time-dependent in cytokine-stimulated endothelial cells in culture. Cell Tissue Res. 284, 415–423.

Schorp, M.K., Tricker, A.R., Dempsey, R., 2012. Reduced exposure evaluation of an Electrically Heated Cigarette Smoking System. Part 1: non-clinical and clinical insights. Regul. Toxicol. Pharmacol. 64, S1–10.

Smyth, G.K., 2004. Linear models and empirical bayes methods for assessing differential expression in microarray experiments. Stat. Appl. Genet. Mol. Biol. 3.

Stocker, C.J., Sugars, K.L., Harari, O.A., Landis, R.C., Morley, B.J., Haskard, D.O., 2000. TNF-alpha, IL-4, and IFN-gamma regulate differential expression of P- and E-selectin expression by porcine aortic endothelial cells. J. Immunol. 164, 3309–3315.

Su, Y., Han, W., Giraldo, C., De Li, Y., Block, E.R., 1998. Effect of cigarette smoke extract on nitric oxide synthase in pulmonary artery endothelial cells. Am. J. Respir. Cell Mol. Biol. 19, 819–825.

Thomson, T.M., Sewer, A., Martin, F., Belcastro, V., Frushour, B.P., Gebel, S., Park, J., Schlage, W.K., Talikka, M., Vasilyev, D.M., Westra, J.W., Hoeng, J., Peitsch, M.C., 2013. Quantitative assessment of biological impact using transcriptomic data and mechanistic network models. Toxicol. Appl. Pharmacol. 272, 863–878.

Wang, Y., Wang, L., Ai, X., Zhao, J., Hao, X., Lu, Y., Qiao, Z., 2004. Nicotine could augment adhesion molecule expression in human endothelial cells through macrophages secreting TNF-alpha, IL-1beta. Int. Immunopharmacol. 4, 1675–1686.

Werley, M.S., Freelin, S.A., Wrenn, S.E., Gerstenberg, B., Roemer, E., Schramke, H., Van Miert, E., Vanscheeuwijck, P., Weber, S., Coggins, C.R., 2008. Smoke chemistry, in vitro and in vivo toxicology evaluations of the electrically heated cigarette smoking system series K. Regul. Toxicol. Pharmacol. 52, 122–139.

Winkelmann, B.R., von Holt, K., Unverdorben, M., 2009. Smoking and atherosclerotic cardiovascular disease: part I: atherosclerotic disease process. Biomarkers Med. 3, 411–428.

Wright, W.R., Parzych, K., Crawford, D., Mein, C., Mitchell, J.A., Paul-Clark, M.J., 2012. Inflammatory transcriptome profiling of human monocytes exposed acutely to cigarette smoke. PLoS One 7, e30120.

Wu, Z., Irizarry, R.A., Gentleman, R., Murillo, F.M., Spencer, F., 2004. A model based background adjustment for oligonucleotide expression arrays. Working Paper 1. Johns Hopkins University, Dept. of Biostatistics.

Yanbaeva, D.G., Dentener, M.A., Creutzberg, E.C., Wesseling, G., Wouters, E.F., 2007. Systemic effects of smoking. Chest 131, 1557–1566.

Zhang, X., Wang, L., Zhang, H., Guo, D., Zhao, J., Qiao, Z., Qiao, J., 2002. The effects of cigarette smoke extract on the endothelial production of soluble intercellular adhesion molecule-1 are mediated through macrophages, possibly by inducing TNF-alpha release. Methods Find. Exp. Clin. Pharmacol. 24, 261–265.

van Leeuwen, D.M., Gottschalk, R.W., van Herwijnen, M.H., Moonen, E.J., Kleinjans, J. C., van Delft, J.H., 2005. Differential gene expression in human peripheral blood mononuclear cells induced by cigarette smoke and its constituents. Toxicol. Sci. 86, 200–210.

van der Toorn, M., Frentzel, S., De Leon, H., Goedertier, D., Peitsch, M.C., Hoeng, J., 2015a. Aerosol from a candidate modified risk tobacco product has reduced effects on chemotaxis and transendothelial migration compared to combustion of conventional cigarettes. Food Chem. Toxicol. 86, 81–87.

van der Toorn, M., Frentzel, S., Goedertier, D., Peitsch, M., Hoeng, J., De Leon, H., 2015b. A prototypic modified risk tobacco product exhibits reduced effects on chemotaxis and transendothelial migration of monocytes compared with a reference cigarette. Food Chem. Toxicol. 80, 277–286.